

doi:10.3788/gzxb20154406.0604001

4.2 K 硅辐射热太赫兹探测器的响应度校准

郑中信^{1,2}, 余耀^{1,2}, 孙建东¹, 李欣幸¹, 秦华¹, 涂学凑³, 陈健³

(1 中国科学院苏州纳米技术与纳米仿生研究所 中国科学院纳米器件与应用重点实验室, 江苏 苏州 215123)

(2 中国科学院大学, 北京 100049)

(3 南京大学 电子科学与工程学院 超导电子学研究所, 南京 210093)

摘 要:提出一种基于标准黑体辐射源对宽谱太赫兹探测器进行响应度定标的方法. 该方法包含一个直线型校准装置、两个定标流程和相应的模拟程序. 考虑实验室温度、湿度和低通滤波器的透射特性, 用该方法实现了 4.2 K 硅辐射热太赫兹探测器的响应度定标. 对黑体辐射的傅里叶变换光谱进行测试, 验证了定标程序和定标结果. 分析定位了定标装置的三种主要误差来源, 并提出相应的改进措施. 所提定标方法适用于热释电太赫兹探测器、微型辐射热太赫兹探测器等宽谱太赫兹探测器的响应度定标.

关键词:太赫兹; 探测器; 响应度; 黑体; 滤波器; 水汽吸收

中图分类号: O43

文献标识码: A

文章编号: 1004-4213(2015)06-0604001-7

Responsivity Calibration of a 4.2 K Silicon Terahertz Bolometer

ZHENG Zhong-xin^{1,2}, YU Yao^{1,2}, SUN Jian-dong¹, LI Xin-xing¹,
QIN Hua¹, TU Xue-cou³, CHEN Jian³

(1 Key Laboratory of Nanodevices and Applications, Suzhou Institute of Nano-Tech and Nano-Bionics, Chinese Academy of Sciences, Suzhou, Jiangsu 215123, China)

(2 University of Chinese Academy of Sciences, Beijing 100049, China)

(3 Research Institute of Superconductor Electronics (RISE), School of Electronic Science and Engineering, Nanjing University, Nanjing 210093, China)

Abstract: A calibration method based on a standard blackbody source for broadband terahertz detectors was proposed. The method includes a line-of-sight calibration setup, two calibration procedures and the corresponding simulation programs. The method takes into account the ambient temperature, the ambient humidity and the transmittance of the terahertz low-pass filter. A 4.2 K silicon bolometer was calibrated in the terahertz range by using the proposed method. The calibrated detector was further verified by using a Fourier-transform spectrometer to measure the blackbody emission spectrum. Three main sources of calibration error were identified and the corresponding solutions to reduce the error were proposed. The method can be applied for terahertz pyroelectric detectors, terahertz microbolometers and other types of broadband terahertz detectors in general.

Key words: Terahertz wave detector; Silicon bolometer calibration; Responsivity; Blackbody radiation; Filter; Water vapor absorption

OCIS Codes: 040.2235; 230.5160; 260.3090; 350.2450; 350.561.

Foundation item: The National Natural Science Foundation of China (Nos. 61271157, 11403084 and 61401456), China Postdoctoral Science Foundation (No. 2014M551678), Jiangsu Planned Projects for Postdoctoral Research Funds (No. 1301054B)

First author: ZHENG Zhong-xin (1984-), male, Ph. D. candidate, mainly focuses on terahertz emission devices. Email: zzxzheng2010@sinano.ac.cn

Responsible author (Corresponding author): QIN Hua (1972-), male, professor, Ph. D. degree, mainly focuses on solid-state terahertz devices and applications. Email: hqin2007@sinano.ac.cn

Received: Jan. 16, 2015; **Accepted:** Mar. 9, 2015

<http://www.photon.ac.cn>

0 Introduction

Terahertz (THz) technology is finding its places in an increasing number of applications^[1-2]. THz detector is one of the key devices for many sensing and detection applications in which not only qualitative but also quantitative analysis of the THz radiation spectrum may be required. The THz spectral responsivity needs to be calibrated for quantitative applications. For example, a calibrated detector is a must for determining the emission power and/or the spectrum of an emitter under development.

To calibrate a detector, the standard-source^[3] method and the standard-detector^[4] method are usually applied. The former method is of fundamental and relies on the standard blackbody source or any calibrated source. The later is of a comparative method and relies on the calibrated detector. Benseman *et al* and Christopher *et al* have used a standard detector to calibrate other un-calibrated detectors^[4]. Steiger *et al* calibrated THz detectors by using both methods^[5]. However, the laboratory environment such as humidity and the ambient temperature are not considered in these calibration procedures. It is well known that severe absorption of THz waves by water takes place.

In this paper, an improved standard source method is proposed to calibrate a silicon bolometer by taking into account both the laboratory temperature and the ambient humidity. The calibration is validated by measuring the blackbody emission spectrum and comparing it to the simulated spectrum.

1 Method

In order to reduce the uncertainties in the calibration, two different procedures are designed to calibrate the responsivity of a 4.2 K silicon bolometer. The corresponding programs are developed to simulate the calibration procedures. The atmospheric model developed at Smithsonian Astrophysical Observatory^[6] is adopted in our simulation programs to calculate the THz absorption by water vapor and the temperature effect. After the responsivity calibration, the detector is implemented in a Fourier transform spectrometer and verified by comparing the measured blackbody emission spectrum with the simulation.

1.1 Setups

1.1.1 Setup for responsivity calibration

The calibration setup is schematically shown in Fig. 1. The calibrated blackbody source and the silicon bolometer to be calibrated are mounted on an optical table in a line-of-sight configuration. The liquid-helium cooled silicon bolometer was manufactured by Infrared Laboratories with a serial number of 3343. The Winston cone of the silicon bolometer faces the center of the blackbody source^[5,7]. The blackbody source (HFY-206B) is produced by Shanghai Fuyuan Optoelectronic Technology Co., Ltd. As stated in the menu, the emissivity of the source is up to 0.99, and the maximum temperature is 900°C. It is worth noting that the blackbody source has a flat emission surface which is 23 cm behind its exit port.

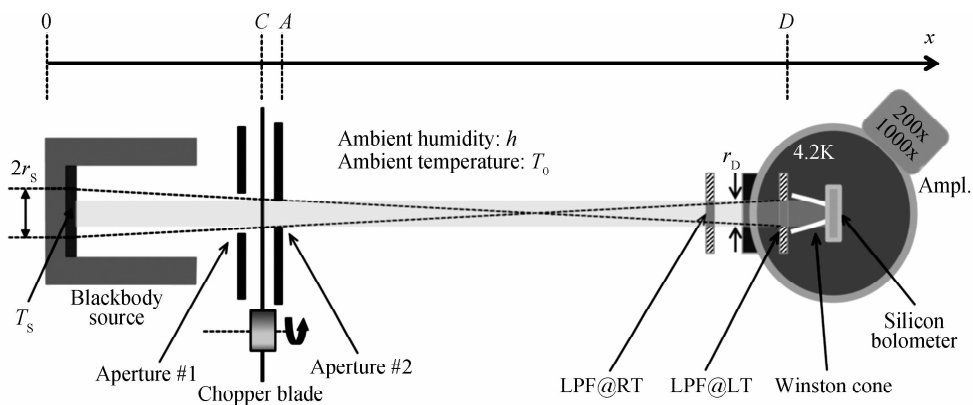


Fig. 1 Schematic setup for the responsivity calibration of a silicon bolometer

A chopper is placed in front of the blackbody source to modulate the emission power. Special cares are taken to stabilize the temperature of the rotating blade by placing two circular apertures in front of and

behind the chopper blade, respectively, as shown in Fig. 1. The diameter of aperture # 1 is smaller than the diameter of blackbody source in order to prevent the chopper blade from being heated^[7], and the

Table 1 Key parameters of the calibration setup

Blackbody temperature $T/^{\circ}\text{C}$	Aperture diameter/mm		X_D/cm	X_C/cm	r_D/mm	Ambient humidity	Ambient temperature/ $^{\circ}\text{C}$
	#1	#2					
200-900	8	6	90-210	30	3	47%	27.8

aperture # 2 defines the total solid angle of the blackbody source seen by the silicon bolometer through the chopper blade [4-5].

Since the blackbody source has strong infrared emission which can be directly sensed by the silicon bolometer, cares must be taken to filter out the short wavelength emission from the blackbody source. Three different Low-Pass Filters (LPF) have been installed in the silicon bolometer for this purpose. Fig. 2 shows the transmittance characteristics of filter LPF # 1 and LPF # 2 cooled at 4.2 K. LPF # 1 is a 1 mm thick wedged sapphire with one face coated by a 4-8 micro diamond scatted layer and the other face coated by white polyethylene and ZnO. The cut-off frequency is about 11 THz and the transmittance ranges from 0.6 to 0.8. LPF # 2 is a diamond-wedged crystalline quartz with a thickness of 1 mm and one of the faces is coated

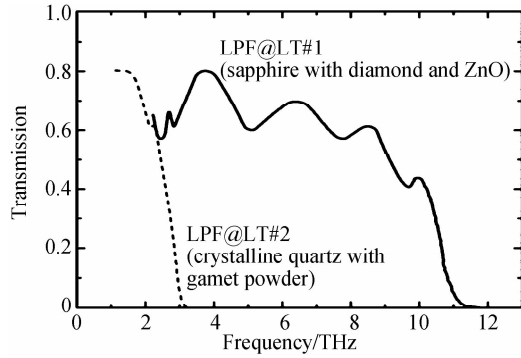


Fig. 2 Transmittance of LPF # 1 and LPF # 2 at 4.2 K in the silicon bolometer

by garnet powder. The cut-off frequency of LPF # 2 is about 2.8 THz, far less than LPF # 1. The transmittance reaches up to 0.8 in the pass band. Experiments have shown that LPFs (LPF @ LT) installed in the silicon bolometer is not as good as that shown in Fig. 2, i. e., significant transmission beyond the cut-off frequencies are observed (data not shown). For this reason, an extra LPF (LPF@RT) made of the same material as that installed in the silicon bolometer is placed in front of the entrance port of the bolometer. The combined LPF@RT and LPF@LT guarantee a negligible transmission beyond the cut-off frequencies.

1.1.2 Setup for spectroscopy of blackbody source

As shown in Fig. 3, the setup for spectroscopy includes a Fourier Transform Spectrometer (FTS), the calibrated silicon bolometer and a blackbody source at 300 K with a background temperature of 7 K. The blackbody radiation is emitted from the chopper blade at 300 K and the emission background is from a cold head cooled down to 7 K. A TPX (Polymethylpentene) window # 1 is installed as the view port of the 7 K cryostat facing to the chopper blade. The chopper modulates the blackbody emission at 37 Hz. The Off-Axis Parabolic mirror (OAP # 1) and the plane mirror collimate the blackbody emission into the FTS. The interference of the two beams from the FTS is

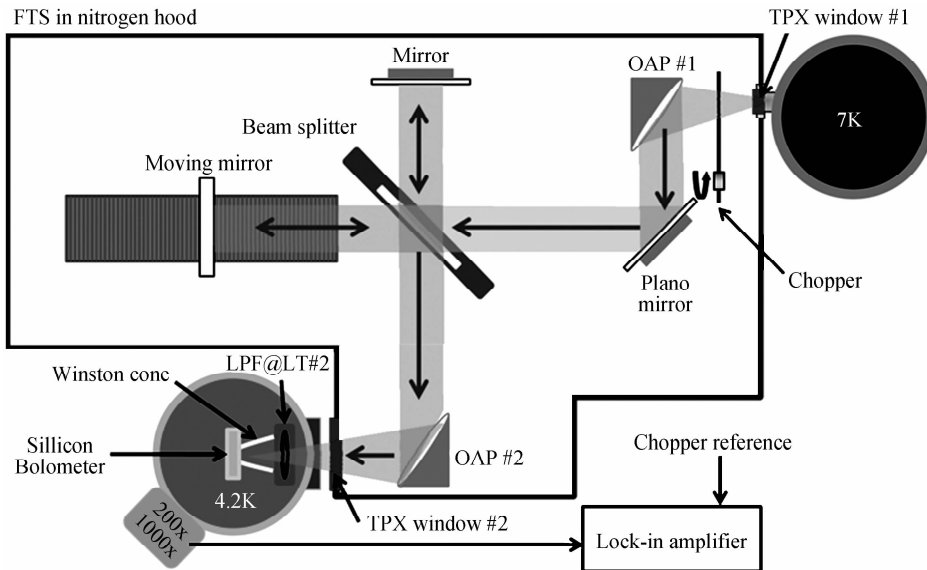


Fig. 3 Spectroscopy of the blackbody emission at 300 K with a background temperature of 7 K by using and the calibrated silicon bolometer

collected by the OAP # 2 and sensed by the silicon bolometer. A TPX window # 2 is installed in front of the silicon bolometer. A dry nitrogen-gas filled hood encloses the whole optical a Fourier-transform spectrometer path except a short beam line (about 2 cm) right between the TPX window # 2 and the Teflon window on the silicon bolometer. By adjusting the plane mirror the blackbody emission is collimated into the FTS for spectroscopy. A lock-in amplifier is used to read out the interferogram by stepping the moving mirror^[5, 8-9]. In the setup, the TPX windows have transmittance of 0.8 in the THz frequency range.

1.2 Model

The broadband emission spectrum from the blackbody is determined by the Planck's law with characteristic parameters such as the temperature and the emissivity^[10-11]. The spectrum is peaked at a characteristic frequency that shifts to higher frequencies with increasing the temperature. The spectral radiance of a blackbody source can be described as

$$B(f, T) = \frac{2hf^3}{c^2} \frac{1}{e^{hf/k_B T} - 1} \quad (1)$$

where, B is the radiation energy per unit time (or the power) per unit area of the emitting surface per unit solid angle per unit frequency from the blackbody in the normal direction, T is the absolute temperature, k_B is the Boltzmann constant, h is the Planck constant and c is the speed of light in vacuum. At room temperature most of the emission is in the infrared region of the electromagnetic spectrum.

A simulation program takes into account the transmittance through the entire optical path and the solid angles seen by the silicon bolometer is developed. In the first step, we consider the overall transmittance of the optical path from the blackbody to the silicon bolometer

$$F(f) = T(f) \times T_i \times V(f) \quad (2)$$

where, $T(f)$ is the transmittance of LPF@RT, T_i is the transmittance of Teflon behind Winston cone, $V(f)$ is the transmittance of the optical path enclosed in the nitrogen hood outside of the cryostat. It is the room temperature and the humidity in the nitrogen hood that determines the transmittance $V(f)$ ^[6].

In the second step, the solid angles of the blackbody source (Ω_{DS}) and the chopper blade (Ω_{DC}) seen by the silicon bolometer are determined as

$$\Omega_{DS} = \frac{\pi r_D^2}{X_D^2} \quad (3)$$

$$\Omega_{DC} = \frac{\pi r_D^2}{(X_D - X_C)^2} \quad (4)$$

where, r_D is the diameter of the opening of the Winston cone, X_C is the distance between the chopper blade and the blackbody source, X_D is the distance between the blackbody source and the Winston cone^[13-14].

In the third step, the total emission power arrives at the silicon bolometer is a sum of that from both the blackbody source and the chopper blade $P = P_{DS} + P_{DC}$ with

$$P_{DS} = A_S \times \Omega_{DS} \times \int_{f_{min}}^{f_{max}} B(f, T_S) \times F(f) df \quad (5)$$

$$P_{DC} = A_C \times \Omega_{DC} \times \int_{f_{min}}^{f_{max}} B(f, T_C) \times F(f) df \quad (6)$$

where, T_S and T_C are the temperature of blackbody and chopper, A_S and A_C are the effective area of the blackbody source and the chopper blade seen by the silicon bolometer, respectively.

In the final step, the output voltage signal from the silicon bolometer can be written as

$$V_D = \alpha \times R_V \times (P_{DS} - P_{DC}) \quad (7)$$

where, R_V is the responsivity of bare silicon bolometer to be calibrated, $\alpha = 0.45$ is determined by the duty cycle of the chopper modulation which is fixed as 50%. Based on the above physical model, a simulation program is developed and allows for simulations of the bolometer signal as a function of the blackbody temperature and the blackbody-bolometer distance.

2 Results and discussion

In order to reduce the uncertainties in the calibration, two different procedures (VT and VD) have been conducted to collect the calibration data. In procedure VT, the bolometer response is measured as a function of the blackbody temperature ($T = 200 - 900^\circ\text{C}$) by keeping the source-detector distance fixed at $X_D = 130\text{cm}$ and all other geometric parameters fixed. In procedure VD, the bolometer response is measured as a function of the source-detector distance ($X_D = 90 - 210\text{cm}$) by keeping the blackbody temperature fixed at $T = 900^\circ\text{C}$ and all other geometric parameters fixed. For both procedures, we measured the bolometer responses when external LPF is switched between LPF@RT # 1 and LPF@RT # 2 while the internal LPF is always fixed as LPF@LT # 2. The main parameters of

the calibration setup and the laboratory environment are listed in Table 1. Once the above experimental calibration data are collected, the target responsivity can be obtained by running the simulations. By implementing the calibrated silicon bolometer in the spectroscopy setup, the calibration model and the programs are verified by comparing to the experimental spectra.

2.1 Responsivity calibration of the silicon bolometer

The results of procedure VD and VT are plotted in Fig. 4 (a) and Fig. 4 (b), respectively. In both procedures, the low pass filter used in the liquid helium cryostat is LPF@LT#2. In procedure VD, the bolometer signals were measured as a function of the source-detector distance by fixing the source temperature at 900°C . The simulated bolometer responses (the dashed curve and the solid curve) agree well with the data points (the open squares and the solid circles) which were obtained by using LPF@RT#1 and LPF@RT#2 as the external filter at room temperature, respectively. The responsivity of the bolometer is obtained as $R_v = 1.1 \times 10^7 \text{ V/W}$. In procedure VT, the source-detector distance is fixed at 130 cm and the source temperature is varied from 200°C to 900°C . Similarly, two sets of data points were obtained by setting the external low-pass filter as

LPF@RT#1 and LPF@RT#2. Simulations with the previously obtained responsivity agree well with both sets of the data points, as shown in Fig. 4 (b). However, it is clear that greater error is observed in procedure VD comparing to procedure VT. This implies that the further the silicon bolometer from the blackbody source, the more accurate the calibration is. Procedures VT alone would be sufficient for responsivity calibration and procedure VD allows for further reducing the calibration error. The responsivity is confirmed by using a backward wave oscillator tuned at 0.9 THz, a calibrated power meter (Model 3A-P-THz from Ophir Optronics Solutions Ltd) and an attenuator (Microtech Instruments Inc.).

2.2 Blackbody spectrum verification

In the above simulations for the calibration procedures, absorption of the THz emission in air has been considered by using the Atmospheric Model(AM) program. The validity of the simulation is examined by comparing the measured blackbody emission spectrum with the simulated spectrum through the air column. The transmission coefficient of THz wave through air is shown in Fig. 5(a). The simulated spectrum and the measured spectrum of a 300 K blackbody are plotted in Fig. 5(b). In the simulation, the length of the optical path in air is set as 200 cm and the humidity is chosen as 47%, both are measured in the laboratory. In the experiment, the external low-pass filter is removed and the only filter inserted in the optical path is the LPF@LT#2. The characteristic absorption lines are marked as A (0.56 THz), B (0.75 THz), C (0.98 THz), D (1.10 THz, 1.16 THz, 1.21 THz), E (1.41 THz), F (1.67 THz), G (2.20 THz), H (2.39 THz) in Fig. 5(a) and are recovered in the spectra shown in Fig. 5(b). These strong absorption lines are from water vapor in air. The absorption induced by water vapor is more than two orders of magnitude stronger than those from oxygen and nitrogen (data not shown). The simulation agrees well with the measured spectra except that the measured transmission in region W is significantly stronger than the simulation, and there is a small deviation in the pass band between the simulation and the experiment. This confirms that LPF@LT#2 is leaky beyond the cut-off frequency and the transmittance in the pass band may be inaccurate. The external low-pass filter is necessary to suppress the transmission in beyond the cut-off frequency.

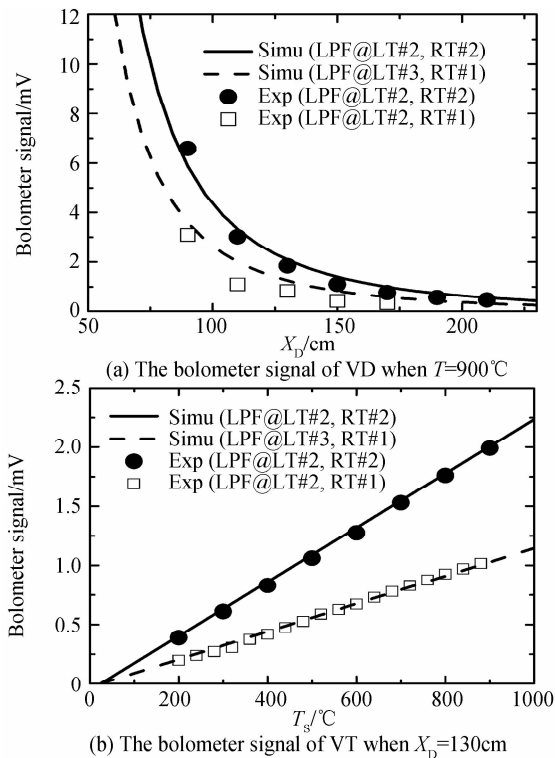


Fig. 4 The results of procedure VD and VT (the symbols are experiment data and the lines are simulation results)

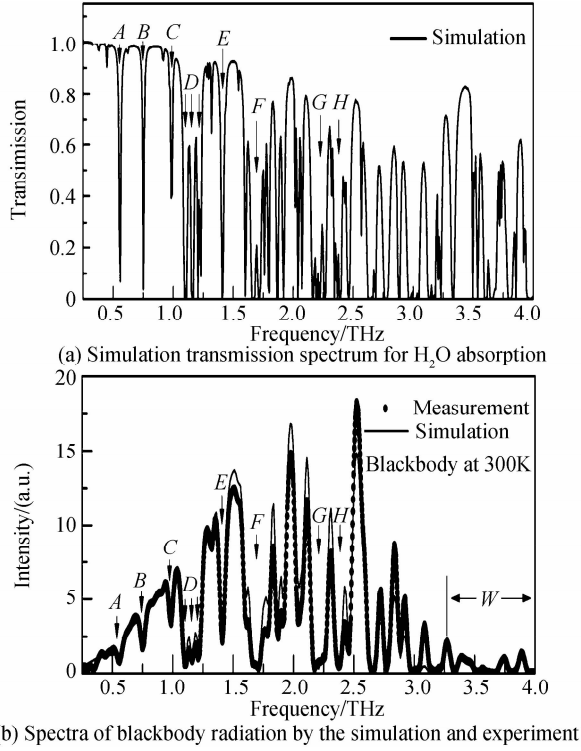


Fig. 5 The comparison of simulation results and measurement results

2.3 Sources of errors in calibration

In the current calibration setup as shown in Fig. 1, there are three sources of errors which can be further reduced. The first is the uncertainty induced by the THz absorption by water vapor [15-16]. The error

Table 2 List of error sources and the induced errors in responsivity calibration

Procedures	Source of errors	Uncertainty	Responsivity error
VD	Humidity	47% ± 5%	-5.3% ~ 4.6%
	Chopper temperature	27.8 ± 3.0 °C	-6.8%
VT	Humidity	47% ± 5%	-5.5% ~ 4.9%
	Chopper temperature	27.8 ± 3.0 °C	-6.6%
	Transmittance of LPF@LT #2	0.3%	0.5%

To reduce the errors, the calibration setup can be improved according to the above mention deficiencies. By filling the optical path with nitrogen gas would allow to minimize and neglect the THz absorption by water vapor. In the optical path at room temperature, insert a low-pass filter with calibrated transmittance and its cut-off frequency lower than that of LPF @ LT # 2 to regulate the blackbody spectrum sensed by the silicon bolometer. To minimize the error introduced by the blackbody emission from the rotating chopper blade, the chopper blade has to be placed as further as possible away from the silicon bolometer and the size of the aperture #2 has to be minimized. A good approach to

comes from the fact that the humidity varies with time in the laboratory and the inaccuracy of the AM program. The second source is from the uncertainty in spectral transmission coefficient of the LPF@LT. The actual transmittance has been proven to be inconsistent with the data provided by the vendor (IR Labs Inc.). Although we have inserted an extra LPF@RT in the optical path, the overall transmittance may be inaccurate. The last source of error comes from the temperature variation on the chopper blade. In the calibration, the temperature of the chopper blade was taken as the room temperature. Although the aperture #1 is implemented to reduce the direct heating of the chopper blade by the nearby blackbody source, the temperature of the chopper blade may be slightly higher than the room temperature and it is difficult to be measured accurately. The variations of the above mentioned sources in current setup and the induced error in the responsivity are listed in Table 2. The relative responsivity error can be written as $\delta = \Delta R_v / R_v = -\Delta P / P$, where $P = P_{DS} - P_{DC}$ and ΔP is the absolute error of power. Both the ambient humidity and the temperature of the chopper blade introduce significant error in the responsivity calibration. It is shown in Table 2 that the maximum error comes from the blackbody emission from the chopper blade.

reduce the amount of blackbody emission from the chopper blade is to collect the blackbody emission from the blackbody source by using a pair of confocal OAPs and place the chopper blade at the focal point. The solid angle of the blackbody source seen by the silicon bolometer needs to be recalculated. It has to be noted that the effect of the temperature on the chopper blade can be neglected when the calibration procedures are applied to a broadband THz detector operated at room temperature.

3 Conclusion

In conclusion, a silicon bolometer is calibrated in the THz frequency range based on a line-of-sight

calibration setup with a standard blackbody source. The obtained responsivity is verified by using a calibrated terahertz power meter and a single frequency continuous-wave THz source. Two procedures together with the corresponding simulation programs are carried out by varying the blackbody temperature and the source-detector distance to obtain a consistent responsivity. The calibrated silicon bolometer is implemented in a Fourier-transform spectrometer for double checking the spectral transmittance of both the air column and the low-pass filter in the optical path. The humidity variation, the transmittance uncertainty of the low-pass filter and the uncertainty in chopper temperature are identified as the main sources of calibration error. The corresponding solutions to reduce the error are proposed. The method reported in the work would become a standard calibration procedure for THz pyroelectric detectors, THz microbolometers and other types of broadband THz detectors in general.

Reference

- [1] FUNK D J, CALGARO F, AVERITT R D, *et al.* THz transmission spectroscopy and imaging: application to energetic materials PBX 9501 and PBX 9502[J]. *Applied Spectroscopy*, 2004, **58**(4): 428-431.
- [2] KEMP M C, TADAY P F, COLE B E, *et al.* Security applications of terahertz technology[C]. SPIE, 2003, **5070**: 44-52.
- [3] GUTSCHWAGER B, MONTE C, DELSIM H H, *et al.* Calculable blackbody radiation as source for the determination of the spectral responsivity of THz detectors[J]. *Metrologia*, 2009, **46**: 165-169.
- [4] BENSEMAN T M, GRAY K E, KOSHELEV A E, *et al.* Powerful terahertz emission from $\text{Bi}_2\text{Sr}_2\text{CaCu}_2\text{O}_{8+\delta}$ mesa arrays[J]. *Applied Physics Letters*, 2013, **103**: 022602.
- [5] STEIGER A, GUTSCHWAGER B, KEHRT M, *et al.* Optical methods for power measurement of terahertz radiation[J]. *Optical Express*, 2010, **18**(21): 21804-21814.
- [6] The AM atmospheric model[CP]. Smithsonian Astrophysical Observatory[2015-01-16]. <https://www.cfa.harvard.edu/~spaine/am/>.
- [7] WERNER L, HUBERS H W, MEINDL P, *et al.* Towards traceable radiometry in the terahertz region[J]. *Metrologia*, 2009, **46**: 160-164.
- [8] RICHARDS P L. Bolometers for infrared and millimeter waves[J]. *Journal of Applied Physics*, 1994, **76**(1): 2-9.
- [9] LI Hong-guang, YANG Hong-ru, YUAN Liang, Terahertz radiation characteristics of blackbody and test method[J]. *Laser & Optoelectronics Progress*, 2013, **50**:071202.
- [10] PLANCK M, MASIUS M, The theory of heat radiation[M]. P. Blakiston's Son & Co, 1914: 9-10.
- [11] SIEGEL R, HOWELL J. Thermal radiation heat transfer [C]. CRC Press Inc, 2002: 8-16.
- [12] CHRISTOPHER W B, NEZIH T Y, MONA J. Responsivity Calibration of Pyroelectric Terahertz Detectors [DB/OL]. ArXiv Physics e-prints 2014, arxiv.org/abs/1412.6878.
- [13] HUANG Yong, CUI Xue, ZHANG Yuan-jun. Probability characteristics of thermal infrared radiation for anisotropic spheres[J]. *Journal of Infrared Millimeter Waves*, 2013, **32**(5): 425-430.
- [14] ZHAN Chun-lian, LI Zheng-qi, LIU Jianp-ping, *et al.* Measurement of spectral irradiance [J]. *Acta Photonica Sinica*, 2009, **38**(5): 1245-1249.
- [15] HUANG Zhuo-lei, WANG Wei-bing, JIANG Wen-jing, *et al.* Infrared detectors with high fill-factor absorber and low offset low out noise readout circuit[J]. *Journal of Infrared Millimeter Waves*, 2014, **33**(1): 50-54.
- [16] CAO Ya-nan, WEI He-li, XU Qing-shan, *et al.* Simulation of atmospheric radiative properties at ir bands under water clouds based on MODIS data[J]. *Acta Photonica Sinica*, 2014, **43**(6): 1-8.